Journal of Colloid and Interface Science 524 (2018) 219–226

Contents lists available at ScienceDirect

Journal of Colloid and Interface Science

journal homepage: www.elsevier.com/locate/jcis

Regular Article

Synthesis of fluorinated graphene oxide by using an easy one-pot deoxyfluorination reaction

Héctor Aguilar-Bolados [a,*], Ahirton Contreras-Cid [b], Mehrdad Yazdani-Pedram [b,*], Gabriela Acosta-Villavicencio [c], Marcos Flores [c], Pablo Fuentealba [b], Andrónico Neira-Carrillo [d], Raquel Verdejo [e], Miguel A. López-Manchado [e]

[a] Facultad de Ciencias Físicas y Matemáticas, Universidad de Chile, Beauchef 850, Santiago, Chile
[b] Facultad de Ciencias Químicas y Farmacéuticas, Universidad de Chile, S. Livingstone 1007, Santiago, Chile
[c] Laboratory of Surfaces and Nanomaterials, Physics Department, Facultad de Ciencias Físicas y Matemáticas, Universidad de Chile, Beauchef 851, Santiago, Chile
[d] Facultad de Ciencias Veterinarias y Pecuarias, Universidad de Chile, Av. Santa Rosa 11735, Santiago, Chile
[e] Instituto de Ciencia y Tecnología de Polímeros, ICTP-CSIC, Juan de la Cierva, 3, 28006-Madrid, Spain

GRAPHICAL ABSTRACT

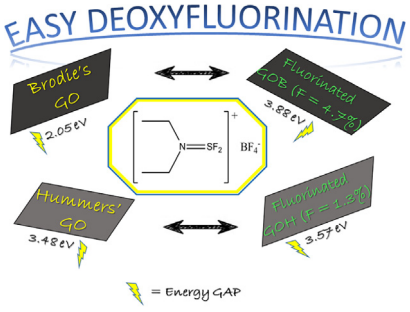

ARTICLE INFO

Article history:
Received 6 March 2018
Revised 4 April 2018
Accepted 5 April 2018
Available online 6 April 2018

Keywords:
Deoxyfluorination reaction
Reconstruction of Csp^2 structure
Fluorinated graphene oxide
Band gap energy

ABSTRACT

The fluorination of two types of graphene oxides conducted by an easy and scalable deoxyfluorination reaction is reported. This reaction was carried out using diethylaminodifluorosulfinium tetrafluoroborate, a stable compound and an efficient reagent for replacing oxygenated functional groups of graphene oxide by fluoride. The graphene oxide produced by the Hummers' method (GOH) showed lower reactivity than that produced by the Brodie's method (GOB). X-ray photoelectron spectroscopy indicated that the highest fluorination degree achieved was 4.7 at.% when GOB was used, and the C—F character corresponds to semi-ionic bonds. Additionally, a partial reduction of GO was concomitant with the functionalization reaction. The deoxyfluorination reaction changed the crystalline structure of GO, favoring the reconstruction of Csp^2 structure of the graphene lattice and reducing the number of stacked layers. The fluorination led to the modification of the electronic band structure of this material, increasing the band gap from 2.05 eV for GOB to 3.88 eV for fluorinated GOB, while for GOH the low flurionation led to a slight increase of the band gap, from 3.48 eV to 3.57 eV.

1. Introduction

The discovery of graphene [1] has meant a revolution in the field of two-dimensional (2D) materials, since this material has

* Corresponding authors.
E-mail addresses: haguilar@ciq.uchile.cl (H. Aguilar-Bolados), myazdani@ciq.uchile.cl (M. Yazdani-Pedram).

https://doi.org/10.1016/j.jcis.2018.04.030
0021-9797/

excellent mechanical properties [2–4], high electrical conductivity (10^7–10^8 S/m) [5] and elevate thermal conductivity (5300 W m^{-1} K^{-1}), which is superior to the those exhibited by diamond (K = 2300 $Wm^{-1}K^{-1}$) [6] and carbon nanotubes (K = 3500 $Wm^{-1}K^{-1}$) [7]. Graphene does not present a gap of energy between its valence and conduction bands, and therefore, graphene is classified as a semi-metallic or zero-gap material [8]. This fact has limited the use of graphene in the manufacture of electronic devices, where semi-conducting materials are used [8,9]. However, there are different strategies to modify the electronic band structure of graphene, seeking the increase of its band gap. These strategies have mainly relied on the covalent functionalization of graphene by halogenation, oxidation and hydrogenation reactions, among others [8–10]. Fluorination is a reaction that leads to a drastic increase of the graphene band gap [8], since the halogen atoms covalently bonded to graphene change the hybridization from sp^2 to sp^3. This has an effect on the local electronic properties of graphene, increasing the difference of energy between the valence and conduction bands [11]. Calculations of band gap values of different halogenated graphenes have been performed using density functional theory (DFT). The resulted values of band gap of fluorinated graphene vary from 3.1 eV [12–14] to 8.3 eV [12,14,15].

To date, several methods for fluorination of graphene have been reported using different starting materials, from graphene films, CVD graphene, graphene oxide, graphite or fluorinated graphite [16]. These methods include direct fluorination [17], plasma fluorination [18], solvothermal fluorination [19–21] or exfoliation by thermal [22] or ultrasonic treatment of fluorinated graphite. Direct fluorination of graphene results in F/C ratio values of up to 1.00 [17]. Nevertheless, these methods are hazardous and complex, requiring special equipment. A simple route for graphene fluorination is the use of graphite oxide as starting materials. For instance, Samanta et al. [21] reported a procedure that used BF_3-etherate and activators, such as 1-heptanethiol or *n*-butylamine to fluorinate graphite oxide. This work was based on the presence on graphite oxide of aryl epoxy groups, which are susceptible to undergo hydrofluorination by ring opening, and on the suitability of BF_3 as a source of nucleophilic fluorine, as it was previously reported by Cresswell et al. [23]. On the other hand, several authors [19,20] have reported the successful fluorination of graphene oxide by reaction with diethylaminosulfur trifluoride (DAST). Although DAST is widely known as a reagent for deoxyfluorination [24], it is an explosive and unstable compound difficult to handle in humid environments [25,26].

A more stable compound, which has been used in deoxyfluorination reactions, is diethylaminodifluorosulfinium tetrafluoroborate (Fig. 1). This compound is more efficient for replacing the oxygenated functional groups by fluorine [27,28]. Diethylaminodifluorosulfinium tetrafluoroborate is a solid reagent, which facilitates scaling up the reaction process [29]. This paper reports, for the first time, the fluorination of graphite oxide by the use of a salt of diethylaminodifluorosulfinium. This deoxyfluorination reaction is simple and easily scalable since it can be carried out using laboratory routine equipment. Moreover, the reactivity of two graphite oxides produced by different oxidation methods is explored.

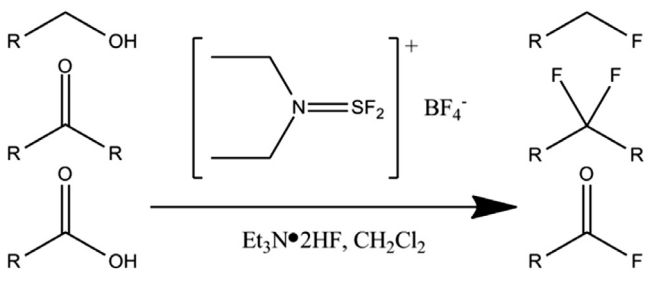

Fig. 1. Deoxyfluorination reaction using tetrafluoroborate of diethylaminodifluorosulfinium.

2. Experimental

2.1. Materials

Natural graphite, fuming nitric acid (99.0%), sulfuric acid (98.0%), potassium chlorate, potassium permanganate, sodium nitrate, hydrogen peroxide (30%), triethylamine, triethylamine trihydrofluoride, diethylaminodifluorosulfinium tetrafluoroborate (XtalFluor-E), dichloromethane, sodium hydrogen carbonate were supplied by Sigma-Aldrich Co., USA, as ACS grade reagents and were used as received.

2.2. Oxidation of graphite

2.2.1. Method of Brödie

5 g of natural graphite were added to 100 ml of fuming nitric acid in a refrigerated reactor (0 °C) and the mixture was left under stirring. Then, 40 g of potassium chlorate were slowly added to the mixture and it was left to react for 22 h. Afterward, the mixture was carefully poured into 1500 ml of cold distilled water. The resulting suspension was centrifuged at 5000 rpm for 5 min. The obtained solid was washed with abundant distilled water. The processes of centrifugation and washing were repeated several times, until it reached pH 7. The obtained solid was dried at 70 °C, for 12 h. The resultant graphite oxide is named GOB.

2.2.2. Method of hummers

2 g of natural graphite, 1 g of sodium nitrate and 44 ml of sulfuric acid (98%) were added to a refrigerated reactor (0 °C) and the mixture was left under stirring. 6 g of potassium permanganate were then carefully added and, heated to 35 °C for 30 min, followed by the addition of 88 ml of distilled water under stirring for 15 min. Afterward a solution of hydrogen peroxide (3%) was added to the suspension until its color changed. The resulting suspension was centrifuged at 5000 rpm for 5 min and the obtained solid was washed with abundant distilled water. This process was repeated several times, until it reached pH 7. The obtained solid was dried at 70 °C, for 12 h. The resultant graphite oxide is named GOH.

2.3. Synthesis of fluorinated graphene oxides

10 g of XtalFluor-E and 87 ml of dichloromethane were added to a thermoregulated two-mouth flask at 0 °C. A mixture of 2.95 g of triethylamine and 9.39 g of triethylamine trihydroflouride was added to the reactor to generate *in situ* triethylamine dihydrofluoride [29]. This mixture was stirred at 0 °C until a homogeneous solution was obtained. Then, 1.46 g of graphite oxide was slowly added and the suspension was left under a continuous nitrogen flow. The resulting solution was left to react at 0 °C for 30 min. Then, the suspension was heated to 25 °C for 20 h. Subsequently, the flask was connected to a reflux system and heated to 40 °C for 2 h. After the reaction time has elapsed, the solution was brought to room temperature and 500 ml sodium hydrogen carbonate (5%) was added to stop the reaction, and the suspension was let under stirring for 15 min. The resulting suspension was centrifuged at 5000 rpm for 5 min and the obtained solid was washed with abundant distilled water. This process was repeated several times. The resulting solid was dried to 70 °C for 12 h. The obtained fluorinated graphene oxides were dialyzed for 96 h using deionized water and a dialysis tubing cellulose membrane (Sigma-

Aldrich Co., US). The fluorinated graphene oxides are named rGOH-F and rGOB-F, depending on the oxidation method used, Hummers or Brodie, respectively.

2.4. Characterization

The chemical composition of different graphitic materials was studied by means of chemical binding energy of the elements, through X-ray photoelectron spectroscopy technique (XPS), using a Perkin Elmer XPS–Auger spectrometer, model PHI 1257 (Massachusetts, USA), which includes an ultra-high vacuum chamber, a hemispheric electron energy analyzer and a X-ray source with Kα radiation unfiltered from an Al ($h\nu$ = 1486.6 eV) anode. The measurements were performed at 400 W and emission angle of 70° to obtain information from the deep surface. The information provided by the C1s spectra is complemented analyzing the O1s spectra, since it is more surface specific than the C1s [30].

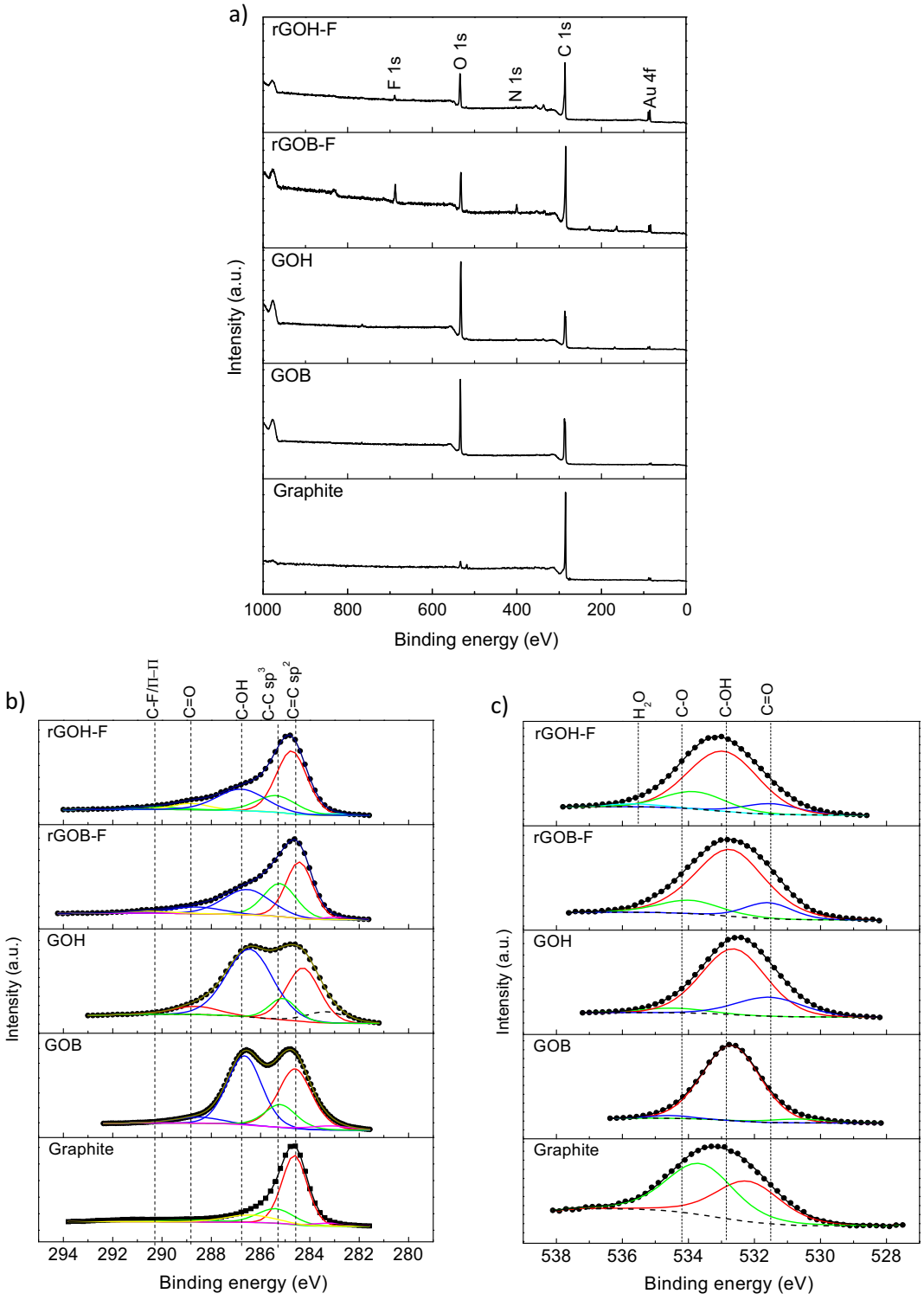

Fig. 2. XPS survey (a), and contributions of the functional groups of C1s (b) and O1s (c) signals of graphene materials.

The graphitic materials were also characterized by Raman spectroscopy using a Renishaw Invia Raman microscope equipped with a 514.5 nm wavelength laser and 0.02 cm^{-1} resolution. The spectra were recorded from 0 to 4000 cm^{-1}. Each Raman spectra were normalized with respect to its highest intensity band. The crystallite sizes (L_a) of different graphitic materials were calculated using Eq. (1) [31].

$$L_a(\mathrm{nm}) = \left(2.4 \times 10^{-10}\right)\lambda^4 \left(\frac{I_D}{I_G}\right)^{-1} \quad (1)$$

where λ is laser wavelength, I_D and I_G are the intensity of *D* and *G* band, respectively.

X-ray diffraction analysis of the graphitic materials was carried out using a Bruker diffractometer model D8 Advance (Massachusetts, USA) with a Cu Kα radiation source, wavelength λ = 0.154 nm and power supply of 40 kV and 40 mA. The incident angle (2θ) was varied between 2° and 80° and the scan rate was 0.02°/s. The interlayer distance (d_{00l}) of graphitic materials was determined by Bragg's law Eq. (2).

$$d_{00l} = \lambda/2sen\theta_{00l} \quad (2)$$

where θ_{00l} is the reflection angle of the reflection plane, and 0 0 l is an integer number.

Solid-state UV spectra were recorded in a Perkin Elmer Lambda 650 equipment coupled with an integration sphere that consist of Praying Mantis™ Diffuse Reflection Accessory and a "Sampling Kit", model DRP-SAP, Harrick Scientific Products, Inc. (New York, USA). Band gap value was estimated by extrapolating the first linear region of the Tauc plots, $(\alpha h\nu)^2$ vs $h\nu$, where α is the absorption coefficient [32].

3. Results and discussion

3.1. X-ray photoelectron spectroscopy

XPS provides information of the different elements present and their atomic ratio from the studied graphitic materials. XPS survey of graphite, GOB, GOH, rGOB-F and rGOH-F are presented in Fig. 2a. The oxidation reaction leads to a significant increase of the oxygen content. The O:C atomic ratios are shown in Table 1, GOH has a higher oxygen content (0.57) as compared to GOB (0.42), which could be attributed to the different nature of the oxidizing species produced during these reactions [33].

After the fluorination reaction, XPS data evidenced both the presence of fluorine and the reduction of the oxygen content. The highest content of fluorine was achieved for GOB obtaining a F:C ratio of 0.06. The C1s and O1s signals were decomposed using a Lorentz function after subtracting a Shirley-type background (Fig. 2b and c and Table 1). The oxidation reaction of graphite introduces carbonyl and hydroxyl/epoxy groups, decreasing the sp^2 signal. Deoxyfluorination reaction produces a significant decrease of hydroxyl/epoxy groups [34]. The contribution of C—F bond could be associated to the signals observed at binding energies 290.5 eV and 290.3 eV present for rGOB-F and rGOH-F, respectively (Fig. 2b). Unfortunately, it is not possible to distinguish between the contributions of the C—F bond and those of the π-π^*, which correspond to shake up satellite peak [34]. Nevertheless, F1s signals provide information of the nature of these bonds. rGOB-F has two contributions at 686.42 eV and 688.03 eV, which indicate that CF bonds have mainly semi-ionic nature. In the case of rGOH-F, the contributions are observed at 687.51 eV and 689.34 eV (Fig. 3), that have a shared character between semi-ionic and covalent [16].

As previously mentioned, rGOB-F has a higher fluorine content than rGOH-F, due probably to the differences of reactivity of the oxygenated functional groups present on both GOs (Table 1). GOB presents a higher content of C—OH groups (93.3 at.%), responsible for the greater conversion of oxygenated functions into fluorine functions. Deoxyfluorination reaction mechanisms have been suggested for simpler organic molecules than GO [28,29]. L'Heureux et al. [28] indicate that Xtalfluor-E reagents effectively convert alcohols to alkyl fluorides and carbonyls to *gem*-difluorides by the

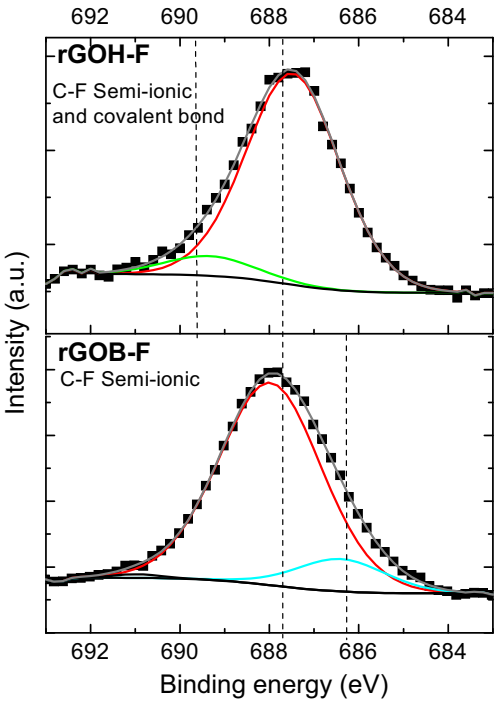

Fig. 3. Contributions of functional groups of F1s signals obtained from XPS analysis of rGOB-F and rGOH-F.

Table 1
Atomic percentage, peak assignment and binding energy for the analyzed samples.

	Atomic percentage (%)					C1s						O1s			
	C	N	O	F	S	C-Au	Sp^2	SP^3	C—OH/C—O—C	C=O	π-π*/C—F	C=O	C—OH	C—O	H_2O
Graphite	96		4			283.0 eV	284.7 eV	285.6 eV	287.3 eV		290.3 eV		532.3	533.7	
						6.0%	53.6%	28.0%	9.5%		3.9%		45.4%	54.6%	
GOB	70		30			283.1 eV	284.7 eV		286.6 eV	288.7 eV		530.7 eV	532.7 eV	534.5 eV	
						3.5%	48.4%		43.9%	4.2%		4.6%	93.1%	2.3%	
GOH	62	1	36		1	283.1 eV	284.5 eV		286.5 eV	288.7 eV		531.6 eV	532.7 eV	534.3 eV	
						3.0%	44.4%		47.0%	5.8%		21.8%	73.3%	5.0%	
rGOB-F	74	4	16	5	1	282.8 eV	284.5 eV	285.4 eV	286.6 eV	288.6 eV	290.5 eV	531.6 eV	532.8 eV	534.0 eV	
						1.5 %	41.8 %	19.8 %	27.2 %	7.2 %	2.6%	11.9%	74.9%	13.2%	
rGOH-F	80		18	1	1	283.0 eV	284.7 eV	285.4 eV	286.7 eV	288.8 eV	290.3 eV	531.6 eV	533. eV 83.3%	534.0 eV	535.3 eV
						1.3 %	48.02 %	16.5%	16.5%	5.6 %	2.9%	6.5 %		6.5%	3.7%

formation of a dialkylaminodifluorsulfane intermediary. Nevertheless, since Xtalfluor-E reactions are fluoride-starved, an exogenous fluoride source is required [28]. This exogenous source corresponds to triethylalmine dihydrofluoride [29], which is *in situ* generated by the previous addition of triethylamine and triethylamine thihydrofluoride to the system.

3.2. Raman spectroscopy

Fig. 4 shows the Raman spectra of the graphitic materials. GOB and GOH present *G* bands shifted to higher frequencies (1581 cm^{-1} and 1591 cm^{-1}, respectively) compared to that observed for graphite (1566 cm^{-1}). This shift is attributed to the fact that the oxidation process leaves some isolated double bonds in the structure and these resonate at higher frequencies [35,36]. The intense bands observed at 1351 cm^{-1} and 1354 cm^{-1} for GOB and GOH, respectively, correspond to the *D* band. The significant increases in the intensity of these bands, compared to graphite, are ascribed to defects in the graphene lattice. These defects could correspond to sp^3-defects, vacancy sites, grain boundaries, among others [37], which appear as a consequence of the graphite oxidation process. The Raman spectrum of rGOH-F does not present important changes compared to that of GOH, since *D* and *G* bands appear at similar Raman shifts, i.e. at 1354 cm^{-1} and 1591 cm^{-1}, respectively. This indicates that the deoxyfluorination reaction does not produce changes in the structure of GOH. Meanwhile, rGOB-F shows significant changes with respect to its corresponding graphene oxide. The *D* and *G* bands are narrower compared to those of GOB, indicating an increase in the crystallinity of the material and, hence, the partial aromatic restoration of the basal plane [35]. This restoration is also reflected in a sensible decrease of the I_D/I_G ratio. However, the presence of the *D'* band suggests the existence of substituent atoms or functional groups at the interface or edges of the crystalline areas [37]. In addition, rGOB-F presents a well-defined second order 2*D* band close to pristine graphite, which originates from in-plane breathing-like mode [38].

These results suggest that the deoxyfluorination reaction leads to a structural modification of the GOB sheets favoring the recovering of graphene lattice. These changes are observed only for the GOB and not for GOH. Hence, GO obtained by different oxidation methods has different reactivity toward the fluorination reaction.

Cançado et al. [31] proposed a general equation to calculate the crystallite size (L_a) of nanographite, which has also been linked to the average interdefect distance by Ferrari et al. [39]. Fig. 4 presents the estimated L_a of the graphitic materials, with a clear reduction of its value after the oxidation process and being this effect more drastic for GOH. This indicates that the Hummers method is a more aggressive method for the oxidation of graphite, compared with Brodie's method, as was previously confirmed by XPS measurements. The deoxyfluorination reaction gives rise to a different behavior depending on the used oxidation method. L_a value of rGOB-F shows a clear increase compared to GOB, whereas this value hardly changes with the fluorination of GOH. Although the oxidation of the graphite is more effective with the Hummers method than with Brodie's method, the latter generates an effective restoration of the sp^2 structure of the graphene lattice with fewer defects. Therefore, GOB is more susceptible than GOH to yield structural changes by the deoxyfluorination reaction.

3.3. X-ray diffraction analysis

Unlike graphite, graphene materials obtained by oxidation reaction or functionalization show a turbostratically stacked layer

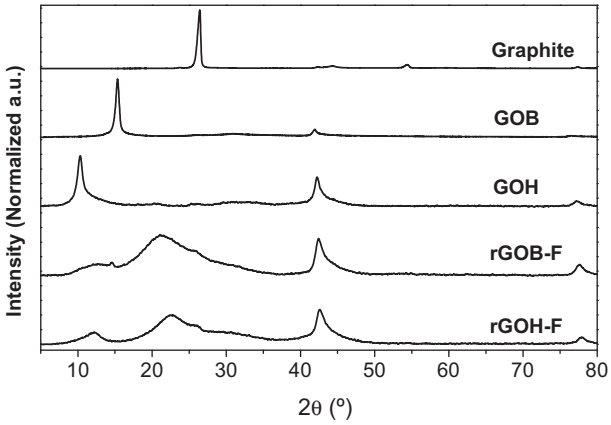

Fig. 5. XRD patterns of graphene materials.

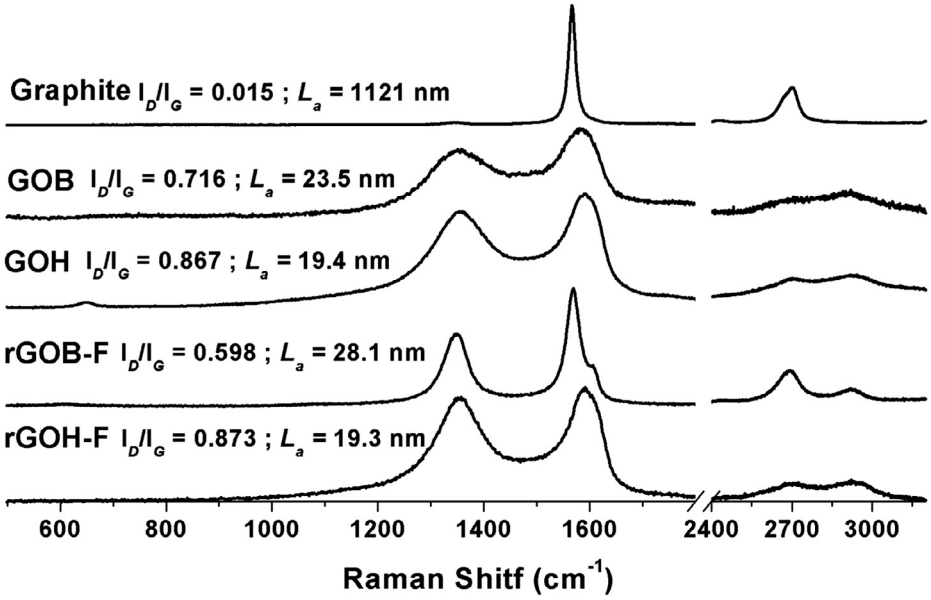

Fig. 4. Raman spectra of graphene materials.

structure. This is reflected in the diffraction patterns, since they contain only (0 0 l) and (h k 0) peaks, without any three-dimensional peak (h k l) (Fig. 5) [40]. The oxidation reaction gives rise to less intense peaks and a shift to lower angles, which results from a change of the long-range order of the crystal structure. Table 2 shows the structural parameters of the graphitic samples. The interlaminar distance was estimated by the Bragg's law and the number of the stacked sheets by the Debye-Scherrer equation, adjusting the reflection peak (0 0 2) to Lorentz curves. Likewise, the average size of crystallites (D) was determined from the (1 0 0) plane reflection [41]. Analysis of the diffraction planes of GOs, showed that these have an average size of crystallites of 31 nm and 12 nm, respectively, being lower than that of the graphite (36 nm). Hence, the oxidation reaction degrades the graphitic structure, being Brodie's method less aggressive. The oxidation reaction also decreases the number of stacked layers [42], from 60 layers for graphite to 30 and 12 layers for GOB and GOH, respectively. On the other hand, the deoxyfluorination reaction further decreases both the average size of crystallites and the number of estimated layers, suggesting an exfoliation process. Therefore, XRD analysis is in agreement with the Raman spectroscopy, having both prove that the Hummers reaction produces larger structural changes than Brödie's, while the deoxyfluorination reaction is more effective on GOB.

3.4. Band structure of graphene oxides and fluorinated graphene oxides

To understand the influence of the oxidation or fluorination reaction in the electronic band structure, the energy band gap of the obtained materials was analyzed (Fig. 6). The corresponding values are summarized in Table 3, where also the band gap values reported in the literature for graphene oxides and fluorinated graphene are shown. A remarkable difference is observed in the values of GOH and GOB, being greater the value for GOH (Fig. 6a). This fact can be explained by the kind of bonds formed in the oxidation procedures: as deduced from XPS, GOH has a larger content of O and C═O bonds, responsible for the increase in the energy gap. This result is consistent with values found in the literature (Table 3).

As already discussed, the fluorination reaction is more effective in GOB, since it produce a higher functionalization degree. This leads to a change of its electronic band structure, where the energy gap increases substantially from 2.05 eV to 3.88 eV (Fig. 6b). However, other authors have reported discrete band gap increases with higher fluoride content [20]. To the best of our knowledge, the deoxyfluorination reaction of GOB favors the reconstruction of the Csp^2 system but the presence of fluorine groups change the local structure of some carbon atoms and, therefore, the electronic properties of the resulting material. This could lead to higher band

Table 2
XRD analysis of the graphene materials.

	Peak (0 0 2)					Peak (1 0 0)		
	2θ (deg)	FWHM (deg)	d (nm)	L_c (nm)	N	2θ (deg)	FWHM	D (nm)
Graphite	26.35	0.43	0.338	20	60	42.35	0.51	36
GOB	15.35	0.51	0.577	17	30	41.63	0.57	31
GOH	10.31	0.86	0.858	9	12	42.35	1.45	12
rGOB-F	12.41	5.32	0.713	2	4	42.28	1.68	10
	21.14	7.20	0.420	1	3			
rGOH-F	12.01	4.17	0.736	2	4	42.79	1.85	9
	22.59	7.75	0.393	1	4			

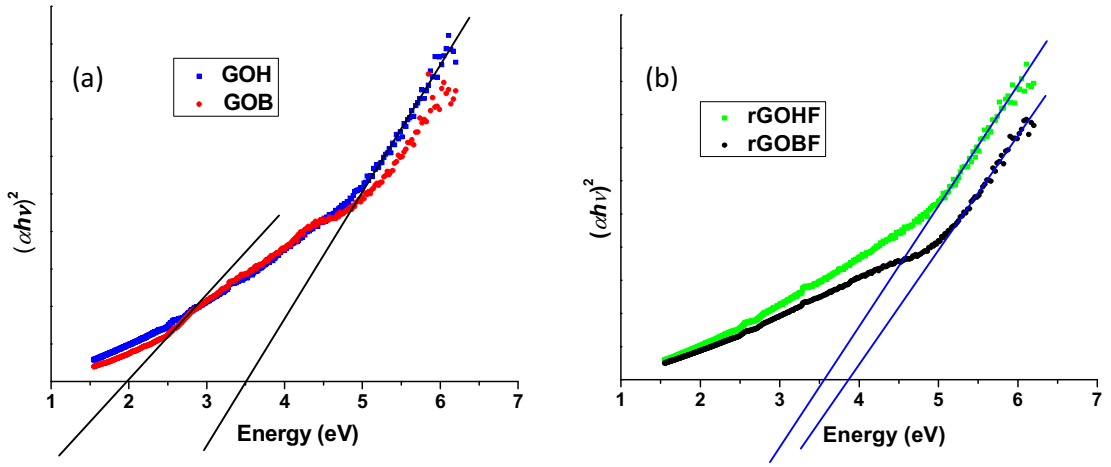

Fig. 6. Tauc plots of studied phases of GOB, GOH, rGOB-F and rGOH-F.

Table 3
Band gap values of graphene oxide and fluorinated graphene oxide.

	GOB	GOH	Fluorinated graphene	rGOB-F	rGOH-F
Band gap reported in literature	2.16 [43]; 1.70–2.40 eV [44]	2.70 eV [45]; 2.90–4.40 eV [46]	2.92–3.10 eV [16]	–	2.73–3.85 eV [20]
Experimental band gap	2.05 eV	3.48 eV	–	3.88 eV	3.57 eV

gap separation [8]. Contrary to these results, rGOH-F has similar band gap separation to that exhibited by its starting material (GOH). The lack of band gap increase could be attributed to low content of fluorine groups found in rGOH-F (1 at.%). This is proved by the Raman spectra of rGOH-F and GOH, which indicate that these materials have similar structures.

4. Conclusions

Fluorinated graphene oxide was successfully prepared through the deoxyfluorination reaction of GO with diethylaminodifluorosulfinioum tetrafluoroborate. Additionally, a partial reduction of GO was concomitant with the functionalization reaction. Two GOs produced by Brodie and Hummers methods were used, showing different reactivity towards deoxyfluorination reaction. Although the oxidation was less effective with the Brodie's method, the resultant GO was more susceptible to yield fluorinated graphene oxides, leading to a higher functionalization degree. The deoxyfluorination reaction changed the crystalline structure of GOB, favoring the reconstruction of Csp^2 structure of the graphene lattice and reducing the number of stacked layers. The incorporation of fluoride groups modified its electronic band structure, increasing its band gap energy. The resulting material can be classified as a semi-conductor and, hence, susceptible to be used in the manufacturing of electronic devices.

Acknowledgements

This research was supported by National Commission for Scientific and Technological Research (CONICYT), Chile, under Postdoctoral fellowship N° 3170104 granted to H. Aguilar-Bolados, Vice Presidency of Research and Development (VID), Universidad de Chile, Chile, under project Enlaces N°ENL010/2017 granted to M. Yazdani-Pedram and Spanish Ministry of Science and Innovation (MICINN), Spain, under project MAT2016-81138-R.

References

[1] K.S. Novoselov, A.K.M. Geim, S.V. Jiang, D. Zhang, Y. Dubonos, S.V. Grigorieva, et al., Electric field effect in atomically thin carbon films, Science 306 (5696) (2004) 666–669.
[2] C. Lee, X.D. Wei, J.W. Kysar, J. Hone, Measurement of the elastic properties and intrinsic strength of monolayer graphene, Science 321 (5887) (2008) 385–388.
[3] M. Poot, H.S.J. van der Zant, Nanomechanical properties of few-layer graphene membranes, Appl. Phys. Lett. 92 (6) (2008) 063111.
[4] A. Vijayaraghavan, Graphene – properties and characterization, in: R. Vajtai (Ed.), Springer Handbook of Nanomaterials, Springer, Berlin, 2013, pp. 39–82.
[5] B. Marinho, M. Ghislandi, E. Tkalya, C.E. Koning, G. de With, Electrical conductivity of compacts of graphene, multi-wall carbon nanotubes, carbon black, and graphite powder, Powder Technol. 221 (2012) 351–358.
[6] A.V. Sukhadolau, E.V. Ivakin, V.G. Ralchenko, A.V. Khomich, A.V. Vlasov, A.F. Popovich, Thermal conductivity of CVD diamond at elevated temperatures, Diam. Relat. Mater. 14 (3–7) (2005) 589–593.
[7] E. Pop, D. Mann, Q. Wang, K.E. Goodson, H.J. Dai, Thermal conductance of an individual single-wall carbon nanotube above room temperature, Nano Lett. 6 (1) (2006) 96–100.
[8] F. Karlický, K. Kumara Ramanatha Datta, Halogenated Graphenes: rapidly growing family of graphene derivatives, ACS Nano 7 (8) (2013) 6434–6464.
[9] R. Balog, B. Jorgensen, L. Nilsson, M. Andersen, E. Rienks, M. Bianchi, M. Fanetti, E. Laegsgaard, A. Baraldi, S. Lizzit, Z. Sljivancanin, F. Besenbacher, B. Hammer, T. G. Pedersen, P. Hofmann, L. Hornekaer, Bandgap opening in graphene induced by patterned hydrogen adsorption, Nat. Mater. 9 (4) (2010) 315–319.
[10] J. Koo, B. Huang, H. Lee, G. Kim, J. Nam, Y. Kwon, H. Lee, Tailoring the electronic band gap of graphyne, J. Phys. Chem. C 118 (5) (2014) 2463–2468.
[11] D.W. Boukhvalov, M.I. Katsnelson, Tuning the gap in bilayer graphene using chemical functionalization: density functional calculations, Phys. Rev. B 78 (8) (2008) 085413.
[12] O. Leenaerts, H. Peelaers, A.D. Hernandez-Nieves, B. Partoens, F.M. Peeters, First-principles investigation of graphene fluoride and graphane, Phys. Rev. B 82 (19) (2010) 195436.
[13] M. Klintenberg, S. Lebegue, M.I. Katsnelson, O. Eriksson, Theoretical analysis of the chemical bonding and electronic structure of graphene interacting with Group IA and Group VIIA elements, Phys. Rev. B 81 (8) (2010) 085433.
[14] F. Karlický, M. Otyepka, Band gaps and optical spectra of chlorographene, fluorographene and graphane from G0W0, GW0 and GW calculations on top of PBE and HSE06 orbitals, J. Chem. Theory Comput. 9 (9) (2013) 4155–4164.
[15] W. Wei, T. Jacob, Electronic and optical properties of fluorinated graphene: a many-body perturbation theory study, Phys. Rev. B 87 (11) (2013) 115431.
[16] W. Feng, P. Long, Y. Feng, Y. Li, Two-dimensional fluorinated graphene: synthesis, structures, properties and applications, Adv. Sci. 3 (7) (2016) 1500413.
[17] R.R. Nair, W. Ren, R. Jalil, I. Riaz, V.G. Kravets, L. Britnell, P. Blake, F. Schedin, A. S. Mayorov, S. Yuan, M.I. Katsnelson, H.-M. Cheng, W. Strupinski, L.G. Bulusheva, A.V. Okotrub, I.V. Grigorieva, A.N. Grigorenko, K.S. Novoselov, A.K. Geim, Fluorographene: a two-dimensional counterpart of teflon, Small 6 (24) (2010) 2877–2884.
[18] J.T. Robinson, J.S. Burgess, C.E. Junkermeier, S.C. Badescu, T.L. Reinecke, F.K. Perkins, M.K. Zalalutdniov, J.W. Baldwin, J.C. Culbertson, P.E. Sheehan, E.S. Snow, Properties of fluorinated graphene films, Nano Lett. 10 (8) (2010) 3001–3005.
[19] X.G. Gao, X.W. Tang, Effective reduction of graphene oxide thin films by a fluorinating agent: diethylaminosulfur trifluoride, Carbon 76 (2014) 133–140.
[20] F.-G. Zhao, G. Zhao, X.-H. Liu, C.-W. Ge, J.-T. Wang, B.-L. Li, Q.-G. Wang, W.-S. Li, Q.-Y. Chen, Fluorinated graphene: facile solution preparation and tailorable properties by fluorine-content tuning, J. Mater. Chem. A 2 (23) (2014) 8782–8789.
[21] K. Samanta, S. Some, Y. Kim, Y. Yoon, M. Min, S.M. Lee, Y. Park, H. Lee, Highly hydrophilic and insulating fluorinated reduced graphene oxide, Chem. Commun. 49 (79) (2013) 8991–8993.
[22] M. Dubois, K. Guerin, Y. Ahmad, N. Batisse, M. Mar, L. Frezet, W. Hourani, J.L. Bubendorff, J. Parmentier, S. Hajjar-Garreau, L. Simon, Thermal exfoliation of fluorinated graphite, Carbon 77 (2014) 688–704.
[23] A.J. Cresswell, S.G. Davies, J.A. Lee, P.M. Roberts, A.J. Russell, J.E. Thomson, M.J. Tyte, β-Fluoroamphetamines via the stereoselective synthesis of benzylic fluorides, Org. Lett. 12 (13) (2010) 2936–2939.
[24] W.J. Middleton, New fluorinating reagents. Dialkylaminosulfur fluorides, J. Org. Chem. 40 (5) (1975) 574–578.
[25] W.J. Middleton, E.M. Bingham, R.F. Sieloff, E.R. Kennedy, C.R. Johnson, Diethylaminosulfur Trifluoride, Organic Syntheses, John Wiley & Sons, Inc., 2003.
[26] A.H. Fauq, R.P. Singh, D.T. Meshri, Handbook of Reagents for Organic Synthesis-Fluorine Containing Reagents, John Willey & Sons Ltd, England, 2007.
[27] O. Mahé, J.-F. Paquin, Diethylaminodifluorosulfinium Tetrafluoroborate (XtalFluor-E®), Encyclopedia of Reagents for Organic Synthesis, John Wiley & Sons, 2003.
[28] A. L'Heureux, F. Beaulieu, C. Bennett, D.R. Bill, S. Clayton, F. LaFlamme, M. Mirmehrabi, S. Tadayon, D. Tovell, M. Couturier, Aminodifluorosulfinium salts: selective fluorination reagents with enhanced thermal stability and ease of handling, J. Org. Chem. 75 (10) (2010) 3401–3411.
[29] F. Beaulieu, L.P. Beauregard, G. Courchesne, M. Couturier, F. Laflamme, A. L'Heureux, Aminodifluorosulfinium tetrafluoroborate salts as stable and crystalline deoxofluorinating reagents, Org. Lett. 11 (21) (2009) 5050–5053.
[30] D. Yang, A. Velamakanni, G. Bozoklu, S. Park, M. Stoller, R.D. Piner, S. Stankovich, I. Jung, D.A. Field, C.A. Ventrice, R.S. Ruoff, Chemical analysis of graphene oxide films after heat and chemical treatments by X-ray photoelectron and Micro-Raman spectroscopy, Carbon 47 (1) (2009) 145–152.
[31] L.G. Cançado, K. Takai, T. Enoki, M. Endo, Y.A. Kim, H. Mizusaki, A. Jorio, L.N. Coelho, R. Magalhães-Paniago, M.A. Pimenta, General equation for the determination of the crystallite size La of nanographite by Raman spectroscopy, Appl. Phys. Lett. 88 (16) (2006) 163106.
[32] B.D. Viezbicke, S. Patel, B.E. Davis, D.P. Birnie, Evaluation of the Tauc method for optical absorption edge determination: ZnO thin films as a model system, Phys. Status Solidi (b) 252 (8) (2015) 170017010.
[33] C. Botas, P. Álvarez, P. Blanco, M. Granda, C. Blanco, R. Santamaría, L.J. Romasanta, R. Verdejo, M.A. López-Manchado, R. Menéndez, Graphene materials with different structures prepared from the same graphite by the Hummers and Brodie methods, Carbon 65 (2013) 156–164.
[34] A. Ganguly, S. Sharma, P. Papakonstantinou, J. Hamilton, Probing the thermal deoxygenation of graphene oxide using high-resolution in situ X-ray-based spectroscopies, J. Phys. Chem. C 115 (34) (2011) 17009–17019.
[35] K.N. Kudin, B. Ozbas, H.C. Schniepp, R.K. Prud'homme, I.A. Aksay, R. Car, Raman spectra of graphite oxide and functionalized graphene sheets, Nano Lett. 8 (1) (2008) 36–41.
[36] A.C. Ferrari, J. Robertson, Interpretation of Raman spectra of disordered and amorphous carbon, Phys. Rev. B 61 (20) (2000) 14095–14107.
[37] Ryan Beams, Luiz Gustavo Cançado, Lukas Novotny, Raman characterization of defects and dopants in graphene, J. Phys.: Condens. Matter 27 (8) (2015) 083002.
[38] A.C. Ferrari, D.M. Basko, Raman spectroscopy as a versatile tool for studying the properties of graphene, Nat. Nanotechnol. 8 (4) (2013) 235–246.
[39] A.C. Ferrari, Raman spectroscopy of graphene and graphite: disorder, electron–phonon coupling, doping and nonadiabatic effects, Solid State Commun. 143 (1) (2007) 47–57.
[40] S.J. Mu, Y.C. Su, L.H. Xiao, S.D. Liu, T. Hu, H.B. Tang, X-ray diffraction pattern of graphite oxide, Chin. Phys. Lett. 30 (9) (2013) 096101.
[41] L. Stobinski, B. Lesiak, A. Malolepszy, M. Mazurkiewicz, B. Mierzwa, J. Zemek, P. Jiricek, I. Bieloshapka, Graphene oxide and reduced graphene oxide studied by the XRD, TEM and electron spectroscopy methods, J. Electron Spectrosc. Related Phenomena 195 (Suppl. C) (2014) 145–154.

[42] S.H. Huh, X-ray diffraction of multi-layer graphenes: instant measurement and determination of the number of layers, Carbon 78 (Suppl. C) (2014) 617–621.
[43] H. Aguilar-Bolados, D. Vargas-Astudillo, M. Yazdani-Pedram, G. Acosta-Villavicencio, P. Fuentealba, A. Contreras-Cid, R. Verdejo, M.A. López-Manchado, Facile and scalable one-step method for amination of graphene using Leuckart reaction, Chem. Mater. 29 (16) (2017) 6698–6705.
[44] H.K. Jeong, M.H. Jin, K.P. So, S.C. Lim, Y.H. Lee, Tailoring the characteristics of graphite oxides by different oxidation times, J. Phys. D Appl. Phys. 42 (6) (2009) 065418.
[45] M.A. Velasco-Soto, S.A. Pérez-García, J. Alvarez-Quintana, Y. Cao, L. Nyborg, L. Licea-Jiménez, Selective band gap manipulation of graphene oxide by its reduction with mild reagents, Carbon 93 (Suppl. C) (2015) 967–973.
[46] H.-C. Hsu, I. Shown, H.-Y. Wei, Y.-C. Chang, H.-Y. Du, Y.-G. Lin, C.-A. Tseng, C.-H. Wang, L.-C. Chen, Y.-C. Lin, K.-H. Chen, Graphene oxide as a promising photocatalyst for CO_2 to methanol conversion, Nanoscale 5 (1) (2013) 262–268.